LANGMUIR

Interface-Rich Materials and Assemblies

pH and Temperature Dual-Responsive Plasmonic Switches of Gold Nanoparticle Monolayer Film for Multiple Anti-counterfeit

Baoqing Liu, Xuefei Lu, Ze Qiao, Liping Song, Qian Cheng, Jiawei Zhang, Afang Zhang, Youju Huang, and Tao Chen

Langmuir, **Just Accepted Manuscript** • DOI: 10.1021/acs.langmuir.8b02989 • Publication Date (Web): 09 Oct 2018

pH and Temperature Dual-Responsive Plasmonic Switches of Gold Nanoparticle Monolayer Film for Multiple Anti-counterfeit

Baoqing Liu[a,b], Xuefei Lu[a,b], Ze Qiao[a], Liping Song[b,c], Qian Cheng[b,c], Jiawei Zhang[b,c], Afang Zhang[a,*], Youju Huang[b,c,*] and Tao Chen[b,c,*]

[a]Department of Polymer Materials, College of Materials Science and Engineering, Shanghai University, Nanchen Road 333, Shanghai 200444, China.

[b]Key Laboratory of Bio-based Polymeric Materials Technology and Application of Zhejiang Province, Ningbo Institute of Material Technology and Engineering, Chinese Academy of Sciences, Ningbo, 315201, China

[c]University of Chinese Academy of Sciences, 19A Yuquan Road, Beijing 100049, China

*E-mail: azhang@shu.edu.cn. *E-mail: yjhuang@nimte.ac.cn. *E-mail: tao.chen@nimte.ac.cn.

ABSTRACT: Two-dimensional (2D) gold nanoparticle (Au NP) monolayer film possesses a lot of fascinating peculiarities, and has shown promising applications in photoelectrical device, catalysis, spectroscopy, sensor and anti-counterfeiting. Due to localized surface plasmon resonance (LSPR) property predetermined by the nature structure of metal nanoparticle, it is usually difficult to realize reversible LSPR transition of 2D film. In this work, we report on fabrication of a large-area free-standing Au NP monolayer film with dual-responsive switchable plasmonic property using a pH- or thermal-responsive dendronized copolymer as stimuli-sensitive linker. In this system, oligoethylene glycol (OEG)-based dendronized copolymer (named PG1A) with pH- or temperature-sensitivity was firstly modified onto the surface of Au NP. Then, polyethylene glycol dibenzyl aldehyde (PEG-DA) was introduced to interact with the amino moieties from PG1A before the process of oil-water interfacial self-assembly of NPs, resulting in an elastic, robust, pH- or temperature-sensitive interpenetrating network among Au NPs in monolayer films. In addition, the film could exhibit reversibly plasmonic shifts about 77 nm and inherent color changes through varying temperature or pH. The obtained free-standing monolayer film also shows excellent transferable property, which can be easily transferred onto substrates such as plastic mold, PDMS, copper grid, silicon wafer. In virtue of these peculiarities of free-standing property, special plasmonic signal and homologous macroscopic color, the transferred film was primely applied to anticounterfeiting security label with clear color change at the designed spots, providing a new avenue to plasmonic nanodevices with various applications.

KEYWORDS: *gold nanoparticle, monolayer film, interfacial self-assembly, dual-responsive, anticounterfeit*

INTRODUCTION

Localized surface plasmon resonance (LSPR), the collective resonant electronic oscillation, depends on the constitutive material properties of noble metals and the surrounding environment.[1] Self-assembly of gold nanoparticles (Au NPs) into two-dimensional (2D) monolayer films have been a matter of interest in recent years due to a controlled LSPR behavior and tailored optical property originating from quantum confinement in discrete nanoparticles and interparticle coupling.[2-5] 2D Au NP films present great potentials in various fields including photovoltaic devices,[6, 7] metamaterials,[8, 9] analysis,[10-12] sensors,[13-16] surface-enhanced Raman scattering (SERS) spectroscopy[17-19] and security anti-counterfeiting.[20] Many of these applications are benefited from controlled LSPR in a reversible manner, however, it is difficult to endow noble metal NP film with reversibly LSPR property that are predetermined by shapes, sizes and compositions of NPs.[1, 21] In order to realize adjustably plasmonic behavior for advanced applications, efforts have been put into integrating plasmonically active NPs with diversely functional media responsive to external stimulus.[22-26] The choice of responsive materials to modulate LSPR was ascribed to distinctive roles in the plasmonic system. The first case was alteration of dielectric functions with active media, which could induce diverse plasmonic frequency and intensity of NPs in the system.[27, 28] The other significant factor was the plasmonic

interparticle coupling depended on the conformation of responsive media, resulting in different plasmonic behavior altered by external surroundings.[29-31]

To date, numerous relevant reports have attained switchable LSPR property via combining NPs with active materials, and most of these were implemented on the basis of single NP or various aggregations and assembly degree limited in solution.[27, 32, 33] For example, through controlling the refractive index of responsive materials, such as polyaniline (PANI), one of representative electroactive materials exhibited disparate dielectric property between reduced and oxidized states, and plasmonic conversion of NPs could be realized in solution.[27, 34] But the system was limited for further applications of plasmonic materials due to confined environment and requirements on specific devices.[30, 35, 36] As a result, it was desired to design 2D hybrid systems with a tunable plasmonic behavior. Fan *et al.*[37] prepared DNA hybridization-directed anchoring of Au NPs with single layer on glass substrates, and realized reversibly plasmonic behavior due to disparate nanogap regulated by humidity. Tsukruk *et al.*[38] and Baumberg *et al.*[39] reported switchable plasmonic layer in the form of depositing NPs on silicon substrates, where LSPR property was adjusted by altering surrounding dielectric environment. However, these plasmonic layers were inconvenient to transfer, because they have been firmly immobilized on substrates and preventing them from further utilization. Therefore, an effective tactic prevailing in the field of nanomaterial film was self-assembly of NPs at liquid-liquid interface, which could fabricate monolayer film with peculiarly optical property.[13, 40] For example, Hallinan *et al.*[41] showed that optical property of Au NPs self-assembled monolayer films (SAMFs) were tuned by

interparticle spacing with different longitudinal ligands, but the preparation process was time-consuming, complex and high-cost. Baumberg *et al.*[42] realized dynamical switching of plasmonic SAMFs made of core-shell Au NPs@PNIPAM by the repeatable expansion and contraction of thermo-responsive polymer (PNIPAM) to tune nanogaps. Whereas, the SAMFs were fragile when transferred onto substrate due to weak physical interaction between NPs, which has gone against extensive applications of active plasmonic nanomaterials.[43, 44] At present, a lot of efforts have therefore been devoted to fabricate high-performance free-standing SAMFs with easily transferred property.[44-46] Recently, we reported a simple and effective chemical crosslinking strategy to achieve a free-standing Au NP monolayer film at oil-water interface, which could be easily transferred onto different substrates with intact morphology.[47] Therefore, introduction of multi-responsive crosslinker before interfacial self-assembly of NPs would be an ideal way for preparation of large-area, free-standing and multi-responsive films with reversible plasmonic switches.

Here, we report on fabrication of a large-area free-standing Au NPs SAMFs with dual-responsiveness and switchable plasmonic property by introducing PG1A as pH or temperature active linker. Unlike small molecules or other linear polymers, the copolymer PG1A imbedded into SAMFs exhibits three distinctive characteristics. Firstly, copolymer provides a thermally-inducible approach to reversibly tune plasmonic behavior and nanogap of SAMFs via repeatedly contraction and extension of copolymer chains through dehydration and rehydration of dendritic OEGs. Secondly, the amino moieties within the copolymer can interact with aldehyde group of

PEG-DA to form pH-sensitive and stable imine bonds among Au NPs, resulting in highly mechanical strength and modulated plasmonic behavior of SAMFs. Similar, decrosslinking and rupture between copolymer and PEG-DA would bring out as pH varied, causing some significant changes on the distance between adjacent NPs, the refractive index of NPs, and visual color. Thirdly, the inherent color changes of SAMFs related with LSPR shift provide a strategy for conveniently visual detection of anticounterfeiting security label, which could be enhanced the security by multiple-color codes and multiple-plasmonic codes.

EXPERIMENTAL SECTION

Reagents and Materials. Chloroauric acid ($HAuCl_4 \cdot 3H_2O$, 99.9%) was purchased from Sigma-Aldrich. Trisodium citrate dehydrate (≥ 99.0%), tris(hydroxymethyl)-amino-methane (TB, GR), n-hexane (GR) and dichloromethane (DCM), dimethylformamide (DMF), 2-aminoethyl methacrylate hydrochloride (AEMA) were acquired from Sinopharm Chemical Reagent Co. Ltd. (Shanghai). 2,2'-Azobis(2-methylpropionitrile) (AIBN) was from TCI, and ethanol absolute (GR, 99.8%) was obtained from Aladdin. Deionized water was used throughout the experimental process. All other chemicals were analytical grade and used as received without further purification.

Preparation of Au NPs. The Au NPs with diameters of 40 nm were prepared according to our previous report.[48] Briefly, trisodium citrate dehydrate solution (10 mL, 33 mM) was added into boiling deionized water (140 mL) with vigorous stirring and continuous heating for 15 min. Then, fresh $HAuCl_4$ (1 mL, 25 mM) and TB solution (5 mL, 0.1 M) were subsequently added

(time delay 60 s) as the temperature of oil bath was maintained at 137 °C. Afterward, extra $HAuCl_4$ (1 mL, 25 mM) was injected twice (interval of 30 min) when oil bath temperature was reduced to 100 °C after continuous heating for 20 min. The ultimate solution was stored in a freezer, and Au NPs of different nanometers can be acquired by modulating the time and temperature of heating trisodium citrate dehydrate solution.

Synthesis of Dendronized Ligands (PG1A). OEG-based dendritic macromonomer (MG1) and cross-linker dialdehyde-terminated polyoxyethylene (PEG-DA) were synthesized according to previous report.[49, 50] Trithiocarbonate-terminated OEG-based dendronized copolymer (PG1A) were prepared through RAFT polymerization. In brief, MG1 (1 g, 1.42 mmol), AEMA (23.5 mg, 0.142 mmol), trithiocarbonate (5.2 mg, 14.2 μmol), AIBN (0.58 mg, 3.55 μmol) and DMF (0.5 mL) were mixed. After three freeze-pump-thaw cycles with N_2, the mixture was stirred at 65 °C for 9 h. After cooling to room temperature (25 °C), the polymer was dissolved in DCM and purified by silica gel column chromatography with DCM as an eluent.

Functionalization of Au NPs with PG1A. Au NPs were modified with PG1A by ligand exchange. Briefly, as-prepared Au NPs (15 mL) were concentrated at 4700 G for 10 min and the supernatant was replaced with equal deionized water. After that, fresh and cool solution (1 mL) containing 3 mg PG1A and 0.5 mg $NaBH_4$ were added. The ultima solution was slowly stirred for 24 h under the condition of ice bath.

Fabrication of Au NP Monolayer Film. Au NP monolayer film was prepared according to our previous work with little improvement.[47] In brief, the modified Au NPs (16 mL) and

deionized water (8 mL) were added into clean glass culture dish (9 cm in diameter) to fully cover the bottom of culture dish, and then hexane (15 mL) was added onto the top of above solution to form an immiscible water/hexane interface. Afterwards, ethyl alcohol (10 mL) was precisely drop-casted to the interface of water/hexane by using a mechanical syringe pump (0.6 mL/min) and PEG-DA (M_w=1000, 1 mL) was injected into the sub-phase. Ultimately, the culture dish was covered with a glass slide for allowing hexane to slowly evaporate within approximate 60 min.

Dual-Responsive Plasmonic Modulation. Au NPs modified with PG1A self-assembly monolayer film (AuNPs@PG1A-DA SAMFs) was deposited on silicon wafers adopting a standard drop-coating method. After drying naturally for five hours, the plasmonic signals were obtained at dried state. Then, in order to acquire thermal-induced plasmonic behavior, the silicon wafer was dipped into aqueous solution with temperature of 25 ^{o}C for measuring the corresponding UV-vis reflection spectra. Subsequently, the aqueous solution was heated up to 50 ^{o}C and was maintained for ten minutes, the resultant plasmonic signal of the film was measured. In addition, in order to verify the pH-responsive LSPR signature, AuNPs@PG1A-DA SAMFs deposited onto silicon wafer was immersed into hydrochloric acid solution (pH=3, ten minutes) for obtaining the plasmonic signal in acid surrounding. Then, the silicon wafer was washed three times using deionized water, whereas it was immerged into sodium hydroxide solution (pH=10) for ten minutes to acquire corresponding plasmonic signal. Moreover, the reversible LSPR behaviors were modulated through repeatedly changing the temperature and pH of solution.

Characterization. Field emission scanning electron microscope (SEM) was performed on S-4800 (Hitachi, Japan) at an acceleration voltage of 8 kV. Transmission electron microscope (TEM) was performed on a TF-20 electron microscope operating at 200 kV. UV-vis absorption spectra were recorded by virtue of TU-1810 UV-vis spectrophotometer provided by Purkinje General Instrument Co. Ltd. Dynamic light scattering (DLS) measurement was performed by Zetasizer Nano ZS Co. Ltd. ^{1}H NMR spectra were recorded on a Bruker Advance AMX-400 Spectrometer. UV-Vis transmittance measurement was carried out on a PE UV/Vis spectrophotometer (Lambda 35) equipped with a thermo-controlled bath. Fourier transform attenuated total reflection infrared spectrometry (FTIR-ATR) was obtained by Nicolet-6700 Fourier transform infrared spectroscopy. The Gel permeation chromatography (GPC) measurement was implemented by a Waters GPC e2695 instrument. The refractive index of polymer network with 3 mg PG1A and 1 mg PEG-DA was obtained by WAY-2SE digital display abbe refractometer with circulating water bath.

RESULTS AND DISCUSSION

Fabrication of Large-Area Au NP Monolayer Film with Functionalization. The monodisperse Au NPs were synthesized through a co-reduction method using sodium citrate and tris-base,[48] and subsequent self-assembly into large-area monolayer film was obtained by a widely oil-water interfacial self-assembly strategy. A typical TEM image is shown in Figure S1a (Supporting Information) for a classical Au NP monolayer film, which suggests a lot of holes and heterogeneity feature accompanied. This morphology should be owed to weak physical interaction between NPs, which makes it unfavorable to transfer the film in an unbroken way and put into practical application. In addition, plasmonic signature of the film is hardly invariant under the external conditions, such as temperature and pH of solution (Figure S1b, Supporting Information) was altered. Since the property of LSPR is predetermined by the shape, size and composition of NPs,[1, 21] it is hard to realize reversibly plasmonic shifts of self-assembled monolayer films (SAMFs).

In order to achieve multi-responsive plasmonic switches as well as easily-transferred property of SAMFs, we synthesized trithiocarbonate-terminated OEG-based dendronized copolymer as pH- and temperature-sensitive linker between neighbored NPs. The copolymer was prepared through reversible addition-fragmentation chain transfer (RAFT) polymerization by using OEG-based dendritic macromonomer (named MG1) for thermo-responsiveness and aminoethyl methacrylate (AEMA) for providing pH-responsive amino

moieties. As a result, the copolymer inherited thermo-sensitiveness of MG1 and its amino moiety could react with aldehydes group of PEG-DA, forming dynamic covalent linkage of imine bonds (-CH=N-) modulated by pH of solution. The composition of copolymer was analyzed by ^{1}H NMR spectroscopy (Figure S2, Supporting Information), which was basically consistent with previous report.[51] The copolymer with high molecular weights (Mn~7.8×10^{4}) and narrow polydispersity indexes (PDI~1.54) were obtained (measured by GPC with DMF as an eluent). Besides, the thermo-responsive property of PG1A was traced by UV-vis spectroscopy that showed the cloud point at 33 ^{o}C as recorded in Figure S3 (Supporting Information). The copolymer exhibited rapid and reversible phase transition in neutrally aqueous solution, and its phase transition temperature could be conveniently adjusted around physiological temperature.

With the help of this copolymer, a large-area Au NP monolayer film was fabricated at oil-water interface through an effectively and conveniently self-assembled strategy as showed in Figure 1a-d. Briefly, n-hexane was discreetly added into as-synthesized Au NP solution for obtaining immiscible oil-water interface. The solution of PEG-DA was added into the water sub-phase for forming an elastic and robust interpenetrating network among Au NPs in monolayer films. Then, ethanol was precisely injected into the water sub-phase in order to easily trap Au NPs at the interface as their surface charges sharply decreased.[49, 50] PG1A was firstly reduced by sodium borohydride to transfer terminal unit trithiocarbonate group into thiol group, and then

chemisorbed onto the surface of Au NPs.[52] Then, PEG-DA and ethyl alcohol were introduced in order to primely construct functional SAMFs during the process of interfacial NPs self-assembly. The UV-vis spec-

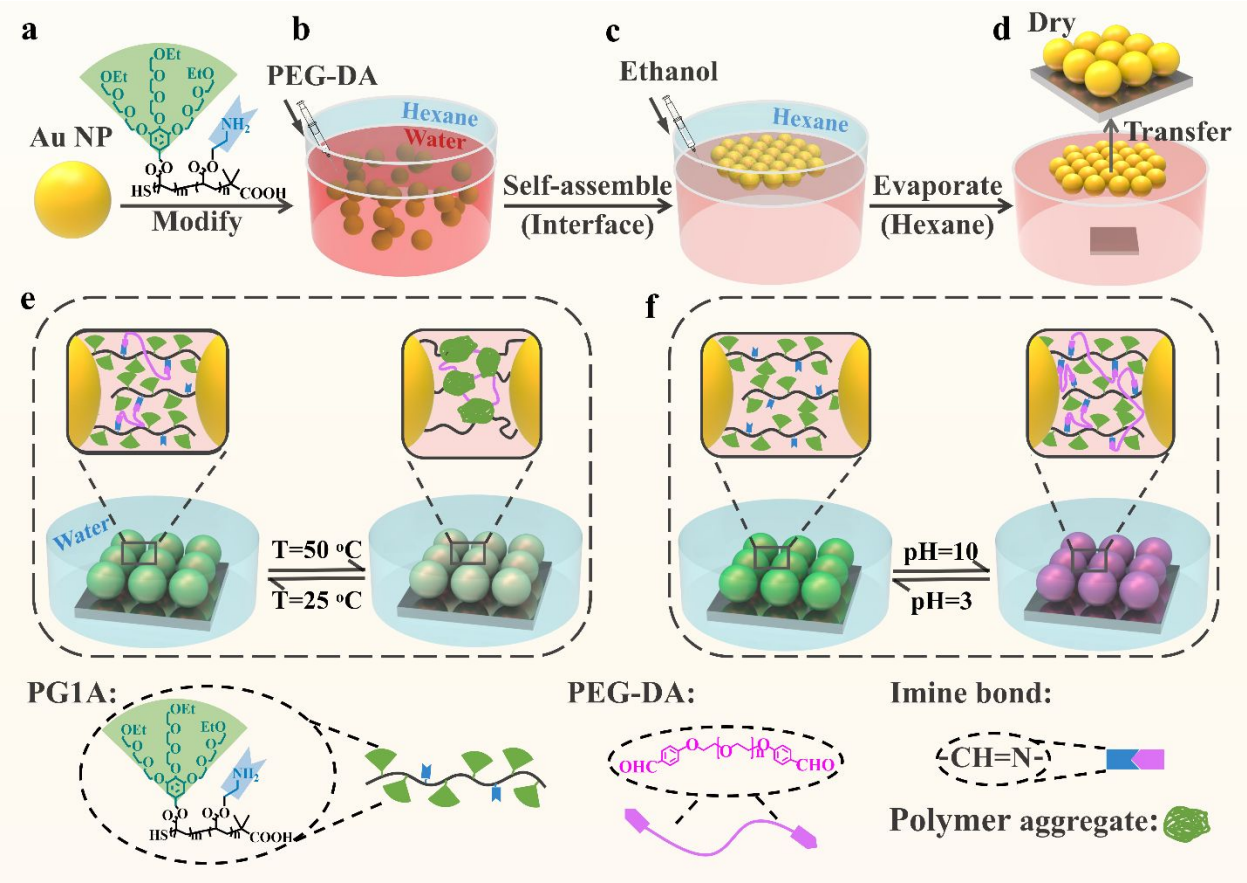

Figure 1. Schematic illustration of the fabrication process of free-standing Au NPs SAMFs at air-water interface. (a) Au NPs modified with PG1A copolymer (Au NPs@PG1A), (b) the solution of PEG-DA was injected into the water sub-phase for forming crosslinked network between NPs (Au NPs@PG1A-DA), (c) ethanol was carefully added into the hexane-water system for trapping Au NPs at interface, (d) evaporation self-assembly and transfer process of interfacial monolayer film, (e, f) multi-responsiveness of SAMFs on silicon wafer under the aqueous solution with different temperature and pH.

tra (Figure S4, Supporting Information) were used to follow the change of Au NP solution before and after modification with thiol-PG1A (for convenience, PG1A was written in full text in place

of thoil-PG1A), whose maximum absorbance peaks were at 518 nm and 522 nm, respectively. The resultant red-shift of 4 nm was relevant with the high molar masses of PG1A and this strongly confirmed that the ligands have been successfully exchanged as reported in literature.[53] In addition, DLS was performed to determine the hydrodynamic diameter of PG1A decorated NPs. Figure S5 (Supporting Information) displayed the intensity-hydrodynamic diameter distributions of Au NPs and Au NPs@PG1A in aqueous solutions. Non-modified Au NPs under different conditions had a lowest *z*-average diameter (D*z)* of 48 nm, whereas Au NPs@PG1A had a Dz of 78 nm at 25 ^{o}C and 823 nm at 50 ^{o}C. The D*z* of Au NPs is smaller than that of Au NPs@PG1A, and remained unaltered with temperature changes, which further proves that the copolymer was successfully decorated onto the surface of NPs. Furthermore, only the D*z* of Au NPs@PG1A could alter with varied temperature. This may be resulted from thermally-induced aggregation of copolymer chains when temperature was elevated above its cloud point,[54] indicating that NPs inherited the thermo-responsiveness of copolymer PG1A.

The SEM images in Figure 2a-b showed that NPs modified with PG1A in the solution had an obvious heterogeneous core-shell nanostructure compared with sodium citrate capped ones, which directly demonstrated Au NPs were successfully modified with PG1A. Moreover, the microstructure of corresponding large-area film (~21 cm^2) after crosslinking by PEG-DA was characterized by SEM and TEM measurements equipped with EDS elemental mapping (displayed in Figure 2c, d). The color of light blue, green, red, orange and yellow of EDS

elemental mapping represents the element of Au, S, C, N and O, respectively. On one hand, S element from an end thiol group of copolymers had a strong interaction Au NP, so it can be easily found that the distribution of S element was on the surface of Au NP, rather than in between nanogap. On the other hand, C, N and O element completely distributed on the surface and among Au NPs, which stemmed from the chain of the copolymer. The element distribution of S, C, N and O indirectly confirmed that PG1A was immobilized on the surface of interfacial Au NPs via Au-S bond and uniformly dispersed amid the nanogaps of SAMFs. In other word, the interparticle spacing would be affected by the conformation of PG1A because of the interpenetrating polymer network within SAMFs, due to the change of the ambient environment.

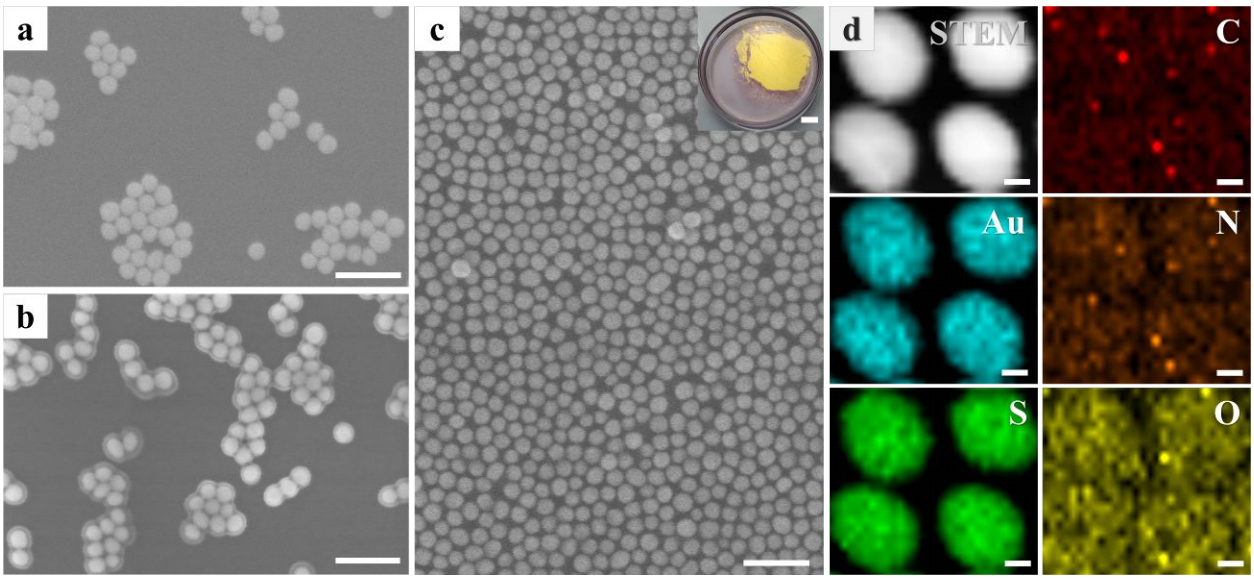

Figure 2. SEM images and elemental evaluation of Au NPs and interfacial Au NP monolayer film. (a-c) SEM images of Au NPs capped with sodium citrate, PG1A copolymer (Au NPs@PG1A) and interfacial self-assembled monolayer films crosslinked by PEG-DA (Au NPs@PG1A-DA SAMFs), respectively. The optical photograph exhibited macroscopic Au NPs@PG1A-DA SAMFs with an area of ~21cm^2. (d) HAADF-STEM (high angle annular dark field image-scanning transmission electron microscope) image and EDS elemental mapping of

Au NPs@PG1A-DA SAMFs. EDS elemental mapping light blue, green, red, orange and yellow color images stand for Au, S, C, N and O element, respectively. The scale bars in a-c, d and optical photo represent 200 nm, 20 nm and 1 cm, respectively.

Cross-linking and Free-standing Monolayer Films. For easily distinguishing the mechanical property of the film, the obtained cross-linked films were studied. Figure 3a showed representative optical photograph of interfacial Au NPs@PG1A-DA SAMF after being transferred. It was clear that the shape of the interfacial monolayer film was unaltered by the change of surface tension and fluctuation after the transfer of film in dashed area, indirectly indicating excellently mechanical property of the SAMF. In order to further characterize the freestanding performance, the microstructures of obtained cross-linked Au NP films were studied with the aid of SEM. A highly matched crack caused by mechanical stress during the transfer process was observed within the Au NPs@PG1A-DA SAMF, indicating the broken way in the form of stiff materials (Figure 3b). This manifests that the film had high free-standing performance due to chemical crosslinking between NPs.[45] It should be noted that, importantly, Au NPs SAMF and Au NPs@PG1A-DA SAMF transferred onto the copper mesh were characterized by SEM (Figure 3c-d). It was clear that the Au NPs SAMF fell in the copper mesh, while the Au NPs@PG1A-DA SAMF covered onto the copper mesh with a broken frizzy configuration. The result further demonstrated the mechanical property of Au NPs@PG1A-DA SAMF, which was consistent with the anticipative peculiarity of free-standing film.[55, 56]

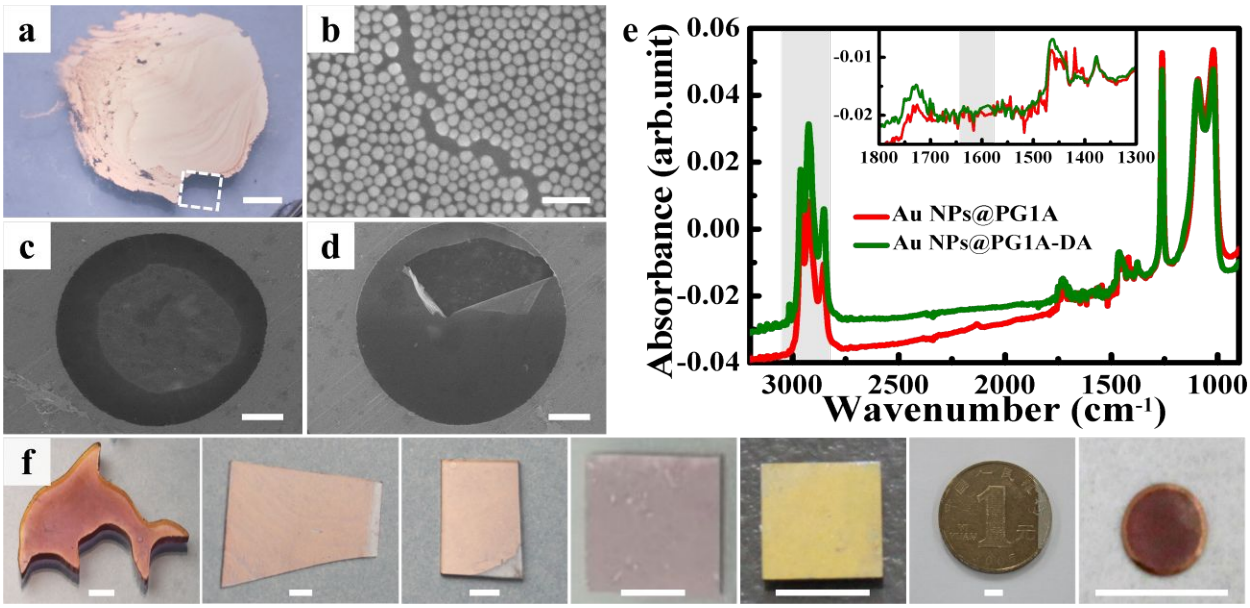

Figure 3. (a) Optical photograph of interfacial Au NPs@PG1A-DA SAMF after being locally transferred. Shape of the interfacial film was unaltered by surface tension and undulation caused by the transfer of film in the dashed line. (b) Microstructure of the crack within the film indicating its broken characteristic in the form of a stiff material. (c, d) SEM images presents undecorated Au NPs SAMF and Au NPs@PG1A-DA SAMF transferred onto the TEM grid, respectively. (e) FTIR-ATR of SAFMs before and after the addition of crosslinker (Au NPs@PG1A and Au NPs@PG1A-DA). (f) Corresponding photographs of Au NPs@PG1A-DA SAMFs transferred onto different substrates: plastic mould, quartz glass, PDMS, filter paper, silicon wafer, coin and copper grid. The scale bars are 5 mm (a, f), 200 nm (b), 10 μm (c, d), respectively.

To understand the chemical crosslinking of covalent linkage between NPs within the film, FTIR-ATR of Au NPs@PG1A-DA SAMF was recorded in Figure 3e. It was observed the diminutive distinction of C=N stretching vibration (ν(C=N)) at 1590 cm^{-1}, revealing the formation of imine bonds between PEG-DA and amino moieties of PG1A. Moreover, the unsaturated =CH stretching vibration (ν(=CH)) at 3015 cm^{-1} was observed after adding PEG-DA into the system, which indirectly proved the formation of imine bonds (-CH=N-). The FTIR-ATR results further demonstrated the free-standing property of Au NPs@PG1A-DA SAMF

causing by the chemical crosslinking of imine linkage. Thus, it was very easy to transfer the free-standing SAMFs with intact shape onto various substrates, such as plastic mould, quartz glass, PDMS, filter paper, silicon wafer, coin and copper grid (showed in Figure 3f), which was beneficial for putting the SAMF into prevailing application of smart window, anti-counterfeiting, plasmonic switch and so on.

Dual-Responsive Plasmonic Switches. Au NPs@PG1A-DA SAMFs were adopted a standard drop-coating method to deposit on silicon wafer and their corresponding UV-vis reflection spectra were listed in Figure 4a. It was obvious that the reflection peak of the film red-shifted from 595 nm at 25 ^{o}C (lower than LCST) to 652 nm at 50 ^{o}C (higher than LCST) in aqueous solution. The remarkable shift of 57 nm should be given the credit to the unique thermo-responsive dendritic OEG structure from PG1A. Owing to reversible phase transition behavior of PG1A, the LSPR shifts could be reversibly modulated at least seven times (Figure 4b), which caused by repeatedly contraction and expansion of polymer chains among Au NPs during surrounding temperature being repeatedly changed between 25 ^{o}C and 50 ^{o}C. In order to clearly explain the mechanism, Figure 5a exhibits the significant parameters that influence the situation of the system, such as the interparticle distance (named d), the height (from the bottom of NPs to the surface of reflective substrate, named h) and the refractive index of SAMFs, which could be reversibly altered owing to conformational transformation of PG1A at various temperature. The

LSPR red-shifted was ascribed to stronger interparticle coupling while the parameters of d and h were decreased as copolymer chains contracted at increased temperature.[42]

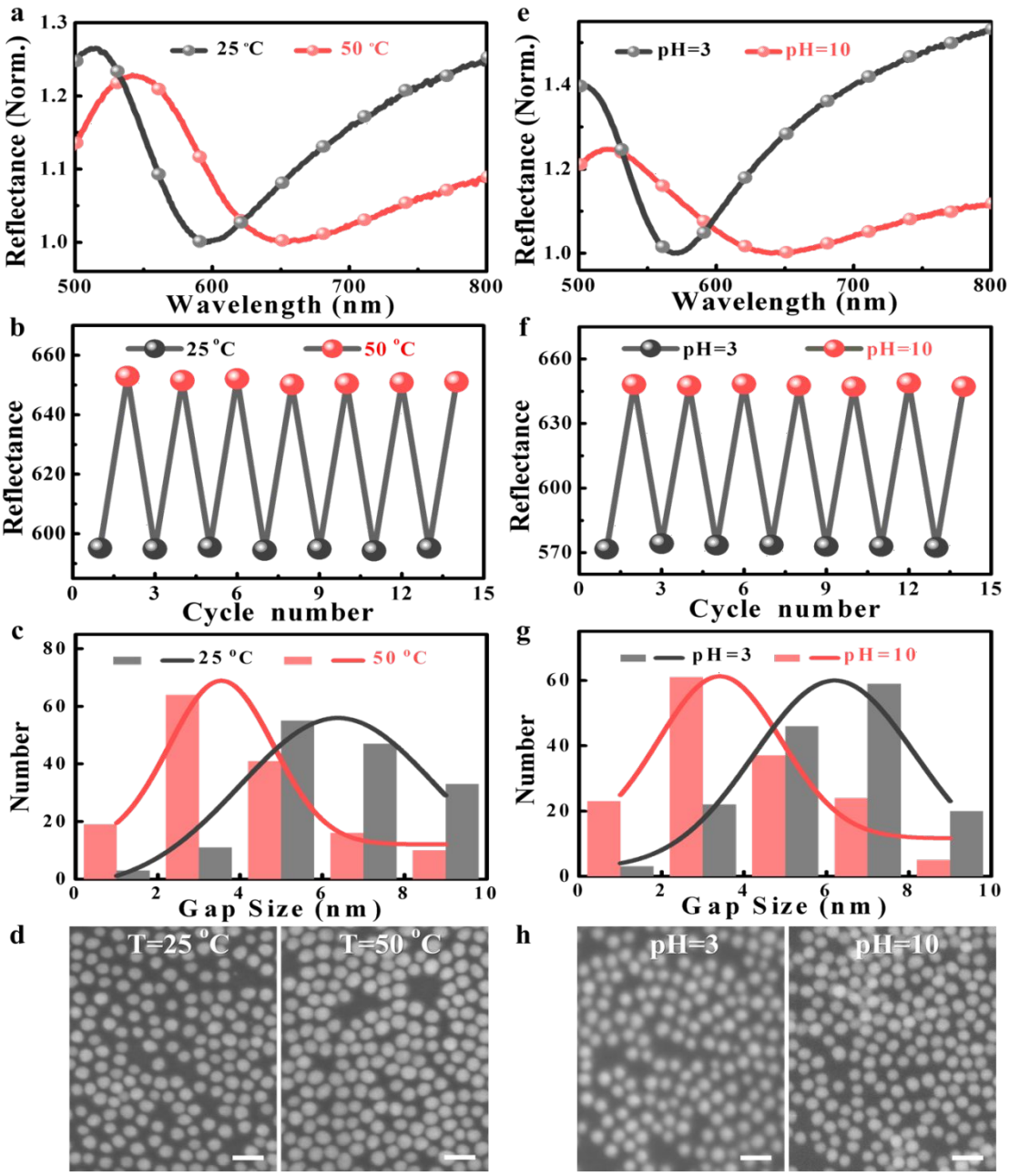

Figure 4. Dual-responsive plasmonic modulation. (a, e) UV-vis reflectance spectrums, (b, f) cycle number of LSPR shift *vs* reflectance, (c, g) corresponding statistical mean nanogaps among neighbored Au NPs and their Gaussian fitting curves, (d, h) SEM characterization of Au

NPs@PG1A-DA SAMFs on silicon wafer under the aqueous solution with diverse temperature and pH. The scare bars are 100 nm.

In order to verify thermally-triggered LSPR behavior of the SAMFs, corresponding microstructure characterizations were implemented and their statistical interparticle spacing were recorded by Nano Measurer (Figure 4c, d). The statistically mean nanogaps within SAMFs dried at 25 ^{o}C and 50 ^{o}C were 6.1 nm and 3.3 nm, which acquired from Gaussian fitting of more than 150 NPs. More remarkable, the same sample was successively used to observe its microstructure after being disposed at various conditions. It was easy to find a more compact arrangement of the film at 50 ^{o}C than the one at 25 ^{o}C. These phenomena indicated that the collapse of polymer chains network resulted in smaller interparticle spacing, because of thermo-triggered aggregation of adjacent NPs at elevated temperature.[54, 57] Moreover, the refractive index of polymer network was obtained by abbe refractometer in circulating water bath. The refractive index value at 25 ^{o}C and 50 ^{o}C were 1.351 and 1.353, respectively. The approximate refractive index demonstrated that the LSPR switches of SAMFs were attributed to plasmonic coupling, which depended on the size of nanogap induced by the conformational change of thermo-sensitive PG1A.

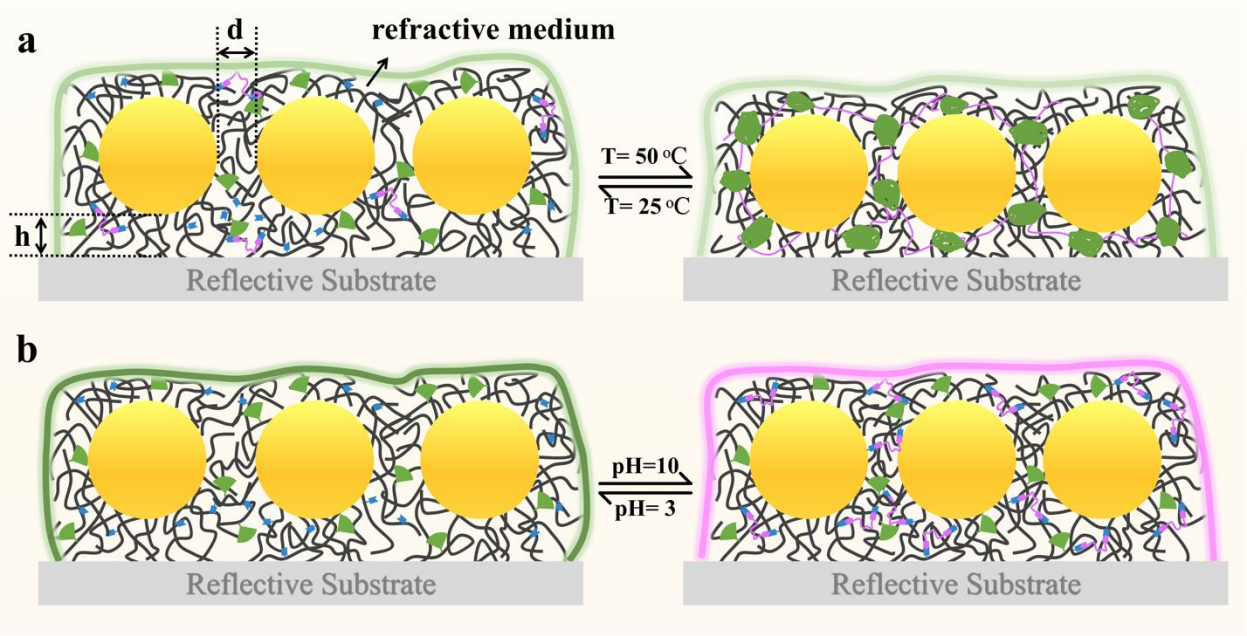

Figure 5. Proposed mechanism illustration of Au NPs@PG1A-DA SAMFs transferred on reflective substrate (silicon wafer) for visual color change under different conditions: 25 °C and 50 °C (a), pH=3 and pH=10 (b).

In addition, UV-vis reflection spectrum, statistically mean nanogaps of more than 150 NPs and SEM image of the film fully displayed the variation of LSPR peaks and nanogap sizes as pH changed (Figure 4e, g, h). The reflection peak value red-shifted from 571 nm in acid solution (pH=3) to 648 nm in base solution (pH=10). The corresponding interparticle spacing diminished from 6.4 nm to 3.5 nm. Because the formation of imine linkage was a dynamic equilibrium process from Schiff-base chemistry,[51] the LSPR shift could be steadily switched at least seven times while pH was repeatedly varied between 3 and 10 (Figure 4f). So large plasmonic shift of 77 nm may be ascribed into strong interparticle coupling of SAMFs as nanogaps narrowed in Figure 4h and Figure 5b, due to the destruction and formation of imine bonds. The formation of imine bonds rendered small nanogap and strong plasmonic interparticle coupling that given rise

to the transfer of plasmonic signal at base condition. And the refractive index of polymer network (measured by abbe refractometer) changed from ~1.345 in acid solution to ~1.375 in base solution. That manifested pH-responsive LSPR switch with so large span was made by differently plasmonic interparticle coupling and the alternation of dielectric surrounding of SAMFs.

Based on above discussion about the dual-responsiveness of the system under various surrounding of aqueous solution, in other words, the interfacial Au NPs@PG1A-DA SAMFs exhibited humidity-responsive LSPR shifts from 628 nm in dry state to 595 nm in aqueous solution at 25 ^{o}C (Figure S6), ascribing to conformational change of PG1A and disparate dielectric environment in air and water. Under the circumstance of elastic and robust polymer network interpenetrates among Au NPs within the film, the interparticle distance was mainly influenced by the state of the copolymer. The copolymer chains would collapse onto the surface of Au NPs caused by strong surface tension during dehydration, whereas they freely stretched through rehydration in the aqueous solution, resulting in enhanced plasmonic coupling with narrow nanogaps and weak plasmonic coupling with stretched nanogaps, respectively. [57]

Multiple-Coded Anti-counterfeit Labels. Considering that the chemical cross-linked AuNPs@PG1A-DA SAMFs possess easily transferrable property and stimuli-responsive plasmonic behaviors, the film could be transferred onto diverse substrates and used to explore interesting and crucial applications. As showed in Figure S7a, a functional AuNPs@PG1A-DA SAMF was deposited on the surface of silicon wafer, then emerged under different ambient

environment. In dry condition, the film showed a kind of homologous macroscopic color of golden yellow. Interestingly, an obvious change of macroscopic color could be discovered after the films being immersed in solvent, from golden yellow (in dry state and in n-hexane) into olive drab (in wet state of aqueous solution) and turquoise (in absolute ethyl alcohol). The phenomena couldn't happen when non-functional Au NPs SAMFs were tested in Figure S7b. The tinctorial transformation of the SAMFs was ascribed to different dielectric environments and plasmonic interparticle coupling caused by the contraction and extension of polymer chains in various surroundings.[9, 24, 25, 37] It could be evidenced from their corresponding reflectance spectrums that the peaks of functional SAMF blue-shifted from ~627 nm (in dried state and in n-hexane) to 595 nm (in aqueous solution) and 586 nm (in absolute ethyl alcohol), whereas, the peaks of non-functional SAMF maintained 647 ~ 643 nm in these conditions. Even more noteworthy is the color of the film changed in aqueous solution and absolute ethyl alcohol because they are good solvent for collapsed PG1A chains to freely stretch, whereas they maintained the same color in n-hexane on account of the insolubility of copolymer. Moreover, the color of AuNPs@PG1A-DA SAMFs could be reversibly changed through repeatedly altering solution surrounding (displayed in Figure 1e, f). An obviously transformative color of the AuNPs@PG1A-DA film changed from olive drab at 25 ^{o}C to celadon at 50 ^{o}C, and from bright green in acid solution (pH=3) to amaranth in base solution (pH=10). Because different intensity of plasmonic coupling and different dielectric environments between adjacent NPs of chromogenic SAMFs, as showed in Figure 4 and Figure 5, were provided by the thermo-triggered conformational change of

dendritic PG1A, the formation and destruction of imine bonds and surrounding refractive index of reflective substrate.

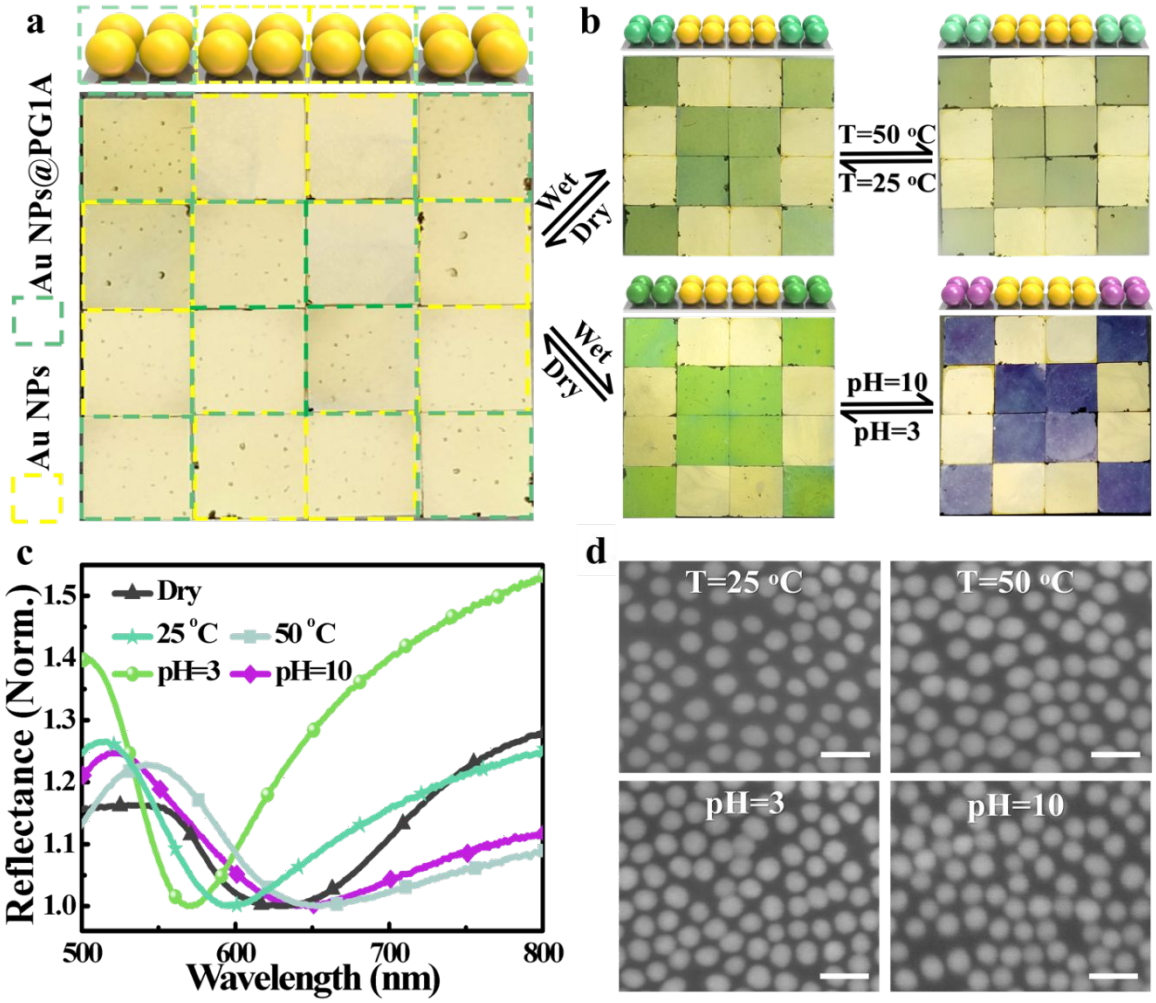

Figure 6. Multiple-coded anti-counterfeit labels. (a) The anti-counterfeit label made up of 16 silicon wafers (0.5 cm×0.5 cm) with transferred Au NPs@PG1A-DA SAMFs and sodium citrate capped Au NPs SAMFs, which displayed alike color acting as "locked code" in the dry state. (b) The label indicated distinguishable color as initially color-coded anti-counterfeiting under the condition of different temperature and pH. (c, d) UV-vis reflectance spectrum and SEM characterization of Au NPs@PG1A-DA SAMFs served as deeply plasmonic code and ultimately microscopic arrangement code. The scale bars are 100 nm.

Hence, to take full advantage of these excellent characteristics of the SAMFs, a simple pattern composed of 16 slices of silicon wafers was designed, half of them were covered with sodium citrate capped Au NPs SAMFs, the rest of them were deposited with functional AuNPs@PG1A-DA SAMFs, as showed in Figure 6a. It was difficult to recognize a hidden pattern and distinguish the difference of SAMFs by naked eye, because they displayed the same macroscopic golden yellow in dried state (acted as "locked code" like an anti-counterfeit label), even though different types of SAMFs were employed. However, a distinctly allochroic pattern within the anti-counterfeit label was visually inspected in solution with different temperature and pH (Figure 6b), which demonstrated the color change of Au NPs@PG1A-DA SAMFs, rather than citrate capped ones. The allochroic pattern made up of 8 slices of silicon wafers with transferred AuNPs@PG1A-DA films, and could be reversibly changed from olive drab to celadon, and from bright green to amaranth through repeatedly altering solution surrounding. These macroscopic discernible colors of SAMFs were convenient to be used as the visual detection of anti-counterfeiting, and consequently were deemed as initially multiple-color codes to estimate the facticity of specimens. As showed in Figure 5 and Figure 6c, the macroscopic color variation of SAMFs was extremely related with their plasmonic behaviors. While the plasmonic signal of the film changed from 628 nm in the dry state to 594 nm (at 25 ^{o}C) and 650 nm (at 50 ^{o}C), to 571 nm (at pH=3) and 643 nm (at pH=10) in wet state, the color of the film changed from golden yellow to olive drab, celadon, bright green and amaranth, respectively. The color and plasmonic behaviors of citrate capped Au NPs film always remained invariable under

these conditions (Figure S1b and Figure 6a, b). Thus, the corresponding LSPR signature of the SAMF could be considered as multiple-plasmonic codes to further verify the reliability of anti-counterfeit label. Moreover, the microscopic arrangements with disparate nanogaps from SEM measurement were determined by the conformational alternation of PG1A and the formation of imine bonds (displayed in Figure 4d, h and Figure 6c), which could be served as ultimately anti-counterfeiting codes to enhance the security of the label. In short, these properties of AuNPs@PG1A-DA SAMFs provide the anti-counterfeit label with multiple-color codes, plasmonic codes and microscopic arrangement codes, effectively enchancing the level of security and providing an expedient approach for safety monitoring.

For exploring the extend circumstance in practical application, we tested the time for stimuli-responsiveness of AuNPs@PG1A-DA SAMFs. When they were immersed in aqueous solution, the color immediately changed within one second, and no more change could be clearly found as time went (Figure S8). It also could be judged by the variation tendency of their corresponding reflective spectrums. Furthermore, the boundary point was significant for thermo-responsiveness, only required the region low or high than critical point, such as 0~31 ^{o}C and 34~80 ^{o}C. As for the pH-responsiveness, vinegar and making soda as daily use could be adopted to regulate pH value of environment. As shown in Figure S9, it can be prepared into various patterns through changing the combination, and was visually inspected in relaxed conditions. These results indicated the possibility to design a new multi-coded safety labels, enhancing the

security and creditability, and paving a convenient way for the quickly visual recognition of anti-counterfeiting.

CONCLUSION

We have successfully fabricated a large-area free-standing monolayer gold nanoparticle film with dual-responsive plasmonic behaviors through a convenient and effective self-assembly strategy at oil-water interface. Through the surface functionalization of gold nanoparticles with OEG-based dendronized copolymers, the free-standing SAMFs exhibited easy-transferred property, and reversible transition of plasmonic signals and switchable chromogenic properties observed with the naked eye. It was found that the conformation of dendritic PG1A, the formation of imine bonds and surrounding refractive index among NPs effected the plasmonic coupling of SAMFs, leading to an obvious color change and a large LSPR shift of 57 nm (different temperature) and 77 nm (different pH). Utilizing multi-chromogenic properties and stimulus-response LSPR behaviors of SAMFs, it is very easy to design multi-coded anti-counterfeit labels. This work would provide opportunities in the construction of large-area free-standing Au nanoparticle monolayer film, SERS based sensors, colorimetric sensor, anticounterfeiting security label and other flexible plasmonic nanodevices.

ASSOCIATED CONTENT

Supporting Information

The Supporting Information is available free of charge on the ACS Publications website.

TEM micrograph and UV-vis reflectance spectrum of the AuNPs SAMF, ^{1}H NMR spectrum and UV-vis transmittance spectrum of OEG-based dendronized copolymer, UV-vis absorption spectrum and dynamic light scattering of Au NPs modified with PG1A. UV-vis reflectance spectra and chromogenic properties of Au NPs@PG1A-DA SAMF and sodium citrate capped Au NPs SAMF in different conditions and the color change of reassembled label.

AUTHOR INFORMATION

Corresponding Authors

*E-mail: azhang@shu.edu.cn

*E-mail: yjhuang@nimte.ac.cn.

*E-mail: tao.chen@nimte.ac.cn.

ACKNOWLEDGMENTS

We gratefully acknowledge the Natural Science Foundation of China (Grant Nos. 51873222, 51473179), the Bureau of Frontier Science and Education of Chinese Academy of Sciences (QYZDB-SSW-SLH036), Fujian province-Chinese Academy of Sciences STS project

(2017T31010024), Ningbo Science and Technology Bureau (2015C110031) and Youth Innovation Promotion Association of Chinese Academy of Science (2016268 and2017337).

REFERENCES

(1) Baffou, G.; Quidant, R., Nanoplasmonics for chemistry. *Chem. Soc. Rev.* **2014**, 43, 3898-3907.

(2) Lee, Y. H.; Shi, W.; Lee, H. K.; Jiang, R.; Phang, I. Y.; Cui, Y.; Isa, L.; Yang, Y.; Wang, J.; Li, S.; Ling, X. Y., Nanoscale surface chemistry directs the tunable assembly of silver octahedra into three two-dimensional plasmonic superlattices. *Nat. Commun.* **2015**, 6, 6990.

(3) Turek, V. A.; Cecchini, M. P.; Paget, J.; Kucernak, A. R.; Kornyshev, A. A.; Edel, J. B., Plasmonic Ruler at the Liquid-Liquid Interface. *ACS Nano.* **2012**, 6, 7789-7799.

(4) Ding, S. Y.; Yi, J.; Li, J. F.; Ren, B.; Wu, D. Y.; Panneerselvam, R.; Tian, Z. Q., Nanostructure-based plasmonenhanced Raman spectroscopy for surface analysis of materials. *Nat. Rev. Mater.* **2016**, 1, 16021.

(5) Shiraishi, Y.; Yasumoto, N.; Imai, J.; Sakamoto, H.; Tanaka, S.; Ichikawa, S.; Ohtani, B.; Hirai, T., Quantum tunneling injection of hot electrons in Au/TiO2 plasmonic photocatalysts. *Nanoscale.* **2017**, 9, 8349-8361

(6) Atwater, H. A.; Polman, A., Plasmonics for improved photovoltaic devices. *Nat Mater.* **2010**, 9, 205-213.

(7) Clavero, C., Plasmon-induced hot-electron generation at nanoparticle/metal-oxide interfaces for photovoltaic and photocatalytic devices. *Nature Photonics.* **2014**, 8, 95-103.

(8) Wang, P.; Gaitanaros, S.; Lee, S.; Bathe, M.; Shih, W. M.; Ke, Y., Programming Self-Assembly of DNA Origami Honeycomb Two-Dimensional Lattices and Plasmonic Metamaterials. *J. Am. Chem. Soc.* **2016**, 138, 7733-7740.

(9) Elbahri, M.; Abdelaziz, M. E.; Homaeigohar, S.; Elsharawy, A.; Keshavarz Hedayati, M.; Roder, C.; El Haj Assad, M.; Abdelaziz, R., Plasmonic Metaparticles on a Blackbody Create Vivid Reflective Colors for Naked-Eye Environmental and Clinical Biodetection. *Adv. Mater.* **2017**, 1704442.

(10) Zhang, L.; Zha, X.; Zhang, G.; Gu, J.; Zhang, W.; Huang, Y.; Zhang, J.; Chen, T., Designing a reductive hybrid membrane to selectively capture noble metallic ions during oil/water emulsion separation with further function enhancement. *J. Mater. Chem. A.* **2018**, 6, 10217-10225.

(11) Zhao, X.; Xu, L.; Sun, M.; Ma, W.; Wu, X.; Xu, C.; Kuang, H., Tuning the interactions between chiral plasmonic films and living cells. *Nature communications* **2017**, 8, 2007.

(12) Li, S.; Xu, L.; Ma, W.; Wu, X.; Sun, M.; Kuang, H.; Wang, L.; Kotov, N. A.; Xu, C., Dual-Mode Ultrasensitive Quantification of MicroRNA in Living Cells by Chiroplasmonic Nanopyramids Self-Assembled from Gold and Upconversion Nanoparticles. *Journal of the American Chemical Society* **2016**, 138, 306-312.

(13) Scanlon, M. D.; Smirnov, E.; Stockmann, T. J.; Peljo, P., Gold Nanofilms at Liquid-Liquid Interfaces: An Emerging Platform for Redox Electrocatalysis, Nanoplasmonic Sensors, and Electrovariable Optics. *Chem. Rev.* **2018**, 118, 3722-3751.

(14) Leem, J.; Wang, M. C.; Kang, P.; Nam, S., Mechanically Self-Assembled, Three-Dimensional Graphene-Gold Hybrid Nanostructures for Advanced Nanoplasmonic Sensors. *Nano Lett.* **2015**, 15, 7684-7690.

(15) Schlicke, H.; Rebber, M.; Kunze, S.; Vossmeyer, T., Resistive pressure sensors based on freestanding membranes of gold nanoparticles. *Nanoscale.* **2016**, 8, 183-186.

(16) Guo, Z.; Jia, Y.; Song, X.; Lu, J.; Lu, X.; Liu, B.; Han, J.; Huang, Y.; Zhang, J.; Chen, T., Giant Gold Nanowire Vesicle-Based Colorimetric and SERS Dual-Mode Immunosensor for Ultrasensitive Detection of Vibrio parahemolyticus. *Anal. Chem.* **2018**, 90, 6124-6130.

(17) Chen, J.; Huang, Y.; Kannan, P.; Zhang, L.; Lin, Z.; Zhang, J.; Chen, T.; Guo, L., Flexible and Adhesive Surface Enhance Raman Scattering Active Tape for Rapid Detection of Pesticide Residues in Fruits and Vegetables. *Anal. Chem.* **2016**, 88, 2149-2155.

(18) Huang, Y.; Ferhan, A. R.; Cho, S. J.; Lee, H.; Kim, D. H., Gold Nanowire Bundles Grown Radially Outward from Silicon Micropillars. *ACS Appl. Mater. Interfaces.* **2015**, 7, 17582-17586.

(19) Huang, Y.; Dai, L.; Song, L.; Zhang, L.; Rong, Y.; Zhang, J.; Nie, Z.; Chen, T., Engineering Gold Nanoparticles in Compass Shape with Broadly Tunable Plasmon Resonances and High-Performance SERS. *ACS Appl. Mater. Interfaces.* **2016**, 8, 27949-27955.

(20) Si, K. J.; Sikdar, D.; Yap, L. W.; Foo, J. K. K.; Guo, P.; Shi, Q.; Premaratne, M.; Cheng, W., Dual-Coded Plasmene Nanosheets as Next-Generation Anticounterfeit Security Labels. *Adv. Optical Mater.* **2015**, 3, 1710-1717.

(21) Liz-Marza´n., L. M.; Murphyc., C. J.; Wang., J., Nanoplasmonics. *Chem. Soc. Rev.* **2014**, 43, 3820-3822.

(22) Liu, A.; Abbineni, G.; Mao, C., Nanocomposite Films Assembled from Genetically Engineered Filamentous Viruses and Gold Nanoparticles: Nanoarchitecture- and Humidity-Tunable Surface Plasmon Resonance Spectra. *Adv. Mater.* **2009**, 21, 1001-1005.

(23) Lee, J.-E.; Chung, K.; Lee, J.; Shin, K.; Kim, D. H., In Situ Studies of Surface-Plasmon-Resonance-Coupling Sensor Mediated by Stimuli-Sensitive Polymer Linker. *Adv. Funct. Mater.* **2015**, 25, 6716-6724.

(24) Ryu, S. H.; Yoon, D. K., Switchable Plasmonic Film Using Nanoconfined Liquid Crystals. *ACS Appl. Mater. Interfaces.* **2017**, 9, 25057-25061.

(25) Ding, T.; Rüttiger, C.; Zheng, X.; Benz, F.; Ohadi, H.; Vandenbosch, G. A. E.; Moshchalkov, V. V.; Gallei, M.; Baumberg, J. J., Fast Dynamic Color Switching in Temperature-Responsive Plasmonic Films. *Adv. Optical Mater.* **2016**, 4, 877-882.

(26) Lee, H.; Jeon, T. Y.; Lee, S. Y.; Lee, S. Y.; Kim, S.-H., Designing Multicolor Micropatterns of Inverse Opals with Photonic Bandgap and Surface Plasmon Resonance. *Adv. Funct. Mater.* **2018**, 1706664.

(27) Jiang, N.; Shao, L.; Wang, J., (Gold nanorod core)/(polyaniline shell) plasmonic switches with large plasmon shifts and modulation depths. *Adv. Mater.* **2014**, 26, 3282-3289.

(28) Ko¨nig., T. A. F.; Ledin., P. A.; Kerszulis., J.; Mahmoud., M. A.; El-Sayed., M. A.; Reynolds., J. R.; Tsukruk., V. V., Electrically Tunable Plasmonic Behavior of Nanocube Polymer Nanomaterials Induced by a Redox-Active Electrochromic Polymer. *ACS Nano.* **2014**, 8 6182-6192.

(29) Karg., M.; Lu., Y.; Carbo-Argibay., E.; Pastoriza-Santos., I.; Pe´rez-Juste., J.; M.Liz-Marza´n., L.; Hellweg., T., Multiresponsive Hybrid Colloids Based on Gold Nanorods and Poly(NIPAM-co-allylacetic acid) Microgels: Temperature- and pH-Tunable Plasmon Resonance. *Langmuir.* **2009**, 25, 3163-3167.

(30) Lv., W.; Liu., S.; Fan., X.; Wang., S.; Zhang., G.; Zhang., F., Gold Nanoparticles Functionalized by a Dextran-Based pH- and Temperature-Sensitive Polymer. *Macromol. Rapid Commun.* **2010**, 31, 454-458.

(31) Qian, Z.; Ginger, D. S., Reversibly Reconfigurable Colloidal Plasmonic Nanomaterials. *J. Am. Chem. Soc.* **2017**, 139, 5266-5276.

(32) Lim, S.; Song, J. E.; La, J. A.; Cho, E. C., Gold Nanospheres Assembled on Hydrogel Colloids Display a Wide Range of Thermoreversible Changes in Optical Bandwidth for Various Plasmonic-Based Color Switches. *Chem. Mater.* **2014**, 26, 3272-3279.

(33) Huang, Y.; Ferhan, A. R.; Kim, D. H., Tunable scattered colors over a wide spectrum from a single nanoparticle. *Nanoscale* **2013**, 5, 7772-5.

(34) Lu, W.; Jiang, N.; Wang, J., Active Electrochemical Plasmonic Switching on Polyaniline-Coated Gold Nanocrystals. *Adv. Mater.* **2017**, 29, 1604862.

(35) Shi, Y.; Selin, V.; Wang, Y.; Sukhishvili, S. A., Multiresponsive Block Copolymer-Modified “Hairy” Gold Nanoparticles for Remote Control of Interfaces. *Part. Part. Syst. Charact.* **2013**, 30, 950-957.

(36) Strozyk, M. S.; Chanana, M.; Pastoriza-Santos, I.; Pérez-Juste, J.; Liz-Marzán, L. M., Protein/Polymer-Based Dual-Responsive Gold Nanoparticles with pH-Dependent Thermal Sensitivity. *Adv. Funct. Mater.* **2012**, 22, 1436-1444.

(37) Shen, J.; Luan, B.; Pei, H.; Yang, Z.; Zuo, X.; Liu, G.; Shi, J.; Wang, L.; Zhou, R.; Cheng, W.; Fan, C., Humidity-Responsive Single-Nanoparticle-Layer Plasmonic Films. *Adv. Mater.* **2017**, 1606796.

(38) Jeon, J.-W.; Zhou, J.; Geldmeier, J. A.; Ponder, J. F.; Mahmoud, M. A.; El-Sayed, M.; Reynolds, J. R.; Tsukruk, V. V., Dual-Responsive Reversible Plasmonic Behavior of Core–Shell Nanostructures with pH-Sensitive and Electroactive Polymer Shells. *Chem. Mater.* **2016**, 28, 7551-7563.

(39) Cormier, S.; Ding, T.; Turek, V.; Baumberg, J. J., Dynamic- and Light-Switchable Self-Assembled Plasmonic Metafilms. *Adv. Optical Mater.* **2018**, 1800208.

(40) Cheng., L.; Aiping Liu; Shuo Peng; Duan., H., Responsive Plasmonic Assemblies of Amphiphilic Nanocrystals at Oil-Water Interfaces. *ACS Nano.* **2010**, 4, 6098-6104.

(41) Yang, G.; Hu, L.; Keiper, T. D.; Xiong, P.; Hallinan, D. T., Jr., Gold Nanoparticle Monolayers with Tunable Optical and Electrical Properties. *Langmuir.* **2016**, 32, 4022-4033.

(42) Ding, T.; Rudrum, A. W.; Herrmann, L. O.; Turek, V.; Baumberg, J. J., Polymer-assisted self-assembly of gold nanoparticle monolayers and their dynamical switching. *Nanoscale.* **2016**, 8, 15864-15869.

(43) Park, Y. K.; Yoo, S. H.; Park, S., Assembly of Highly Ordered Nanoparticle Monolayers at a Water/Hexane Interface. *Langmuir.* **2007**, 23, 10505-10510.

(44) Kosif, I.; Kratz, K.; You, S. S.; Bera, M. K.; Kim, K.; Leahy, B.; Emrick, T.; Lee, K. Y.; Lin, B., Robust Gold Nanoparticle Sheets by Ligand Cross-Linking at the Air-Water Interface. *ACS Nano.* **2017**, 11, 1292-1300.

(45) Andryszewski, T.; Iwan, M.; Hołdyński, M.; Fiałkowski, M., Synthesis of a Free-Standing Monolayer of Covalently Bonded Gold Nanoparticles. *Chem. Mater.* **2016**, 28, 5304-5313.

(46) Free-Standing Bilayered Nanoparticle Superlattice Nanosheets with Asymmetric Ionic Transport Behaviors. *ACS nano* **2015**, 9, 11218–11224.

(47) Lu, X.; Huang, Y.; Liu, B.; Zhang, L.; Song, L.; Zhang, J.; Zhang, A.; Chen, T., Light-Controlled Shrinkage of Large-Area Gold Nanoparticle Monolayer Film for Tunable SERS Activity. *Chem. Mater.* **2018**, 30, 1989-1997.

(48) Lu, X. F.; Dandapat, A.; Huang, Y. J.; Zhang, L.; Rong, Y.; Dai, L. W.; Sasson, Y.; Zhang, J. W.; Chen, T., Tris base assisted synthesis of monodispersed citrate-capped gold nanospheres with tunable size. *RSC Adv.* **2016**, 6, 60916-60921.

(49) Li, W.; Zhang, A.; Schluter, A. D., Thermoresponsive dendronized polymers with tunable lower critical solution temperatures. *Chem. Commun.* **2008**, 5523-5525.

(50) Junk, M. J.; Li, W.; Schluter, A. D.; Wegner, G.; Spiess, H. W.; Zhang, A.; Hinderberger, D., Formation of a mesoscopic skin barrier in mesoglobules of thermoresponsive polymers. *J. Am. Chem. Soc.* **2011**, 133, 10832-10838.

(51) Liu, J.; Zhang, X.; Chen, X.; Qu, L.; Zhang, L.; Li, W.; Zhang, A., Stimuli-responsive dendronized polymeric hydrogels through Schiff-base chemistry showing remarkable topological effects. *Polym. Chem.* **2018**, 9, 378-387.

(52) Lowe., A. B.; Sumerlin., B. S.; Donovan., M. S.; McCormick., C. L., Facile Preparation of Transition Metal Nanoparticles Stabilized by Well-Defined (Co)polymers Synthesized via Aqueous Reversible Addition-Fragmentation Chain Transfer Polymerization. *J. Am. Chem. Soc.* **2002**, 124, 11563.

(53) Haiss., W.; Thanh., N. T. K.; Jenny Aveyard; Fernig., D. G., Determination of Size and Concentration of Gold Nanoparticles from UV-Vis Spectra. *Anal. Chem.* **2007**, 79, 4215-4221.

(54) Gillich., T.; Acikgo., C.; Isa., L.; Schlu¨ter., A. D.; Spencer., N. D.; Textor., M., PEG-Stabilized Core-Shell Nanoparticles: Impact of Linear versus Dendritic Polymer Shell Architecture on Colloidal Properties and the Reversibility of Temperature-Induced Aggregation. *ACS Nano.* **2013**, 7, 316-329.

(55) Jiang, Z.; He, J.; Deshmukh, S. A.; Kanjanaboos, P.; Kamath, G.; Wang, Y.; Sankaranarayanan, S. K.; Wang, J.; Jaeger, H. M.; Lin, X. M., Subnanometre ligand-shell asymmetry leads to Janus-like nanoparticle membranes. *Nat Mater.* **2015**, 14, 912-917.

(56) Wang, Y.; Liao, J.; McBride, S. P.; Efrati, E.; Lin, X. M.; Jaeger, H. M., Strong Resistance to Bending Observed for Nanoparticle Membranes. *Nano Lett.* **2015**, 15, 6732-6737.

(57) Gillich, T.; Benetti, E. M.; Rakhmatullina, E.; Konradi, R.; Li, W.; Zhang, A.; Schluter, A. D.; Textor, M., Self-assembly of focal point oligo-catechol ethylene glycol

dendrons on titanium oxide surfaces: adsorption kinetics, surface characterization, and nonfouling properties. *J. Am. Chem. Soc.* **2011**, 133, 10940-10950.

ToC

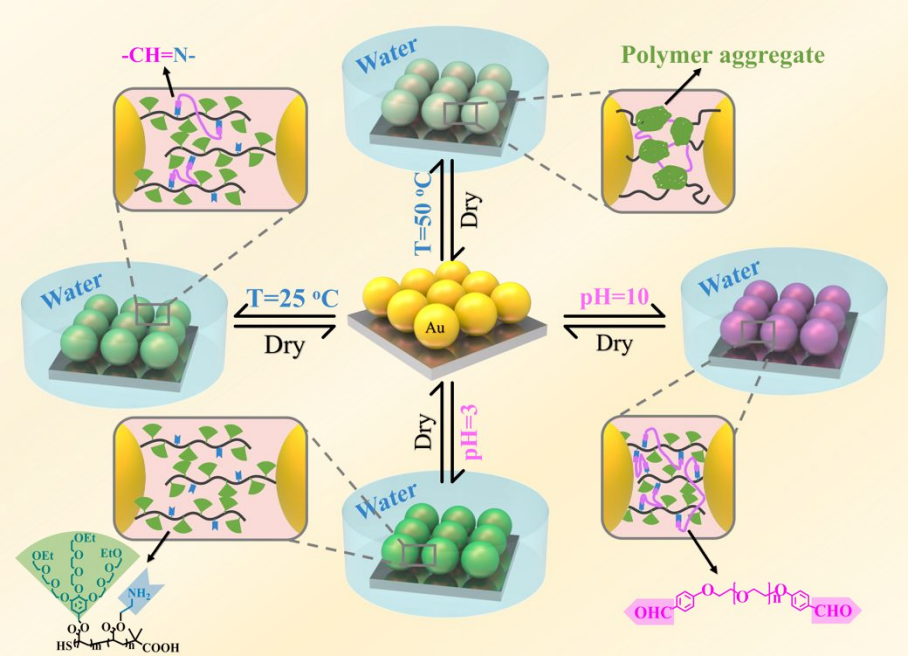
-CH=N-
Water
Polymer aggregate
T=50 °C
Dry
Water
T=25 °C
Dry
Au
pH=10
Dry
Water
Dry
pH=3
Water
OHC
CHO